Published in final edited form as:
Neurobiol Dis. 2009 November ; 36(2): 293–302. doi:10.1016/j.nbd.2009.07.021.

Biochemical and immunohistochemical analysis of an Alzheimer's disease mouse model reveals the presence of multiple cerebral Aβ assembly forms throughout life

Ganesh M. Shankar[1,2], **Malcolm A. Leissring**[2], **Anthony Adame**[3], **Xiaoyan Sun**[2], **Edward Spooner**[2], **Eliezer Masliah**[3], **Dennis J. Selkoe**[2], **Cynthia A. Lemere**[2], and **Dominic M. Walsh**[1,*]

[1]Laboratory for Neurodegenerative Research, School of Biomolecular and Biomedical Sciences, Conway Institute for Biomedical and Biomolecular Research, University College Dublin, Republic of Ireland [2]Department of Neurology, Harvard Medical School and Center for Neurologic Diseases, Brigham and Women's Hospital, Boston, MA 02115 [3]Department of Neurosciences, School of Medicine, University of California, La Jolla, San Diego, CA92093

Abstract

The amyloid β-protein (Aβ) is believed to play a causal role in Alzheimer's disease, however, the mechanism by which Aβ mediates its' effect and the assembly form(s) of Aβ responsible remain unclear. Several APP transgenic mice have been shown to accumulate Aβ and to develop cognitive deficits. We have studied one such model, the J20 mouse. Using an immunoprecipitation/Western blotting technique we find an age-dependent increase in Aβ monomer and SDS-stable dimer. But prior to the earliest detection of Aβ dimers, immunohistochemical analysis revealed an increase in oligomer immunoreactivity that was coincident with reduced hippocampal MAP2 and synaptophysin staining. Moreover, biochemical fractionation and ELISA analysis revealed evidence of TBS and triton-insoluble sedimentable Aβ aggregates at the earliest ages studied. These data demonstrate the presence of multiple assembly forms of Aβ throughout the life of J20 mice and highlight the difficulty in attributing synaptotoxicity to a single Aβ species.

Keywords

Amyloid β-protein; aggregation; oligomers; amyloid precursor protein; J20 mice; synaptophysin; MAP2

INTRODUCTION

Alzheimer's disease (AD) histopathology of the cerebral cortex is characterized by an accumulation of amyloid plaques containing the amyloid β-protein (Aβ) and neurofibrillary

*Correspondence to: Dominic M. Walsh, Laboratory for Neurodegenerative Research, The Conway Institute for Biomolecular and Biomedical Research, University College Dublin, Belfield, Dublin 4, Republic of Ireland, dominic.walsh@ucd.ie, Tel: 353-1-716 6751, Fax: 353-1-716 6890.

tangles composed of hyperphosphorylated tau (Mirra et al., 1991). Yet plaques and tangles are not unique to AD (Terry et al., 1987; 2001) and while the number and distribution of tangles shows a moderate correlation with severity of disease (Braak and Braak, 1997; Schonheit et al., 2004), amyloid burden is a less robust indicator (Dickson, 1997; 2001; Bennett et al., 2006). Nonetheless, considerable experimental data suggests that Aβ plays an important role in AD pathogenesis (Selkoe, 2001). For instance, in the brains of humans affected by AD the concentration of aqueous-soluble Aβ predicts the clinical severity of dementia better than either amyloid plaque or neurofibrillary tangle density (Kuo et al., 1996; McLean et al., 1999; Lemere et al., 2002). Parallel *in vitro* studies have revealed that soluble oligomeric forms of synthetic Aβ perturb synaptic structure and activity and impair learning and memory whereas Aβ monomer has no adverse effect (Lambert et al., 1998; Hartley et al., 1999; Wang et al., 2002; Klyubin et al., 2004; Wang et al., 2004; Lacor et al., 2007; Puzzo et al., 2008). Together, these *ex vivo* and *in vitro* studies have lead to a revision of the amyloid cascade hypothesis; wherein, soluble Aβ oligomers are the primary neurotoxic agents in AD (Klein et al., 2001; Hardy and Selkoe, 2002). However, the precise identity of these species and their relationship with amyloid plaques still remains unclear (Walsh and Selkoe, 2007).

Transgenic mouse models over-expressing various forms of human APP develop amyloid pathology, certain synaptic changes, electrophysiological deficits and impairment of learning and memory relevant to AD (Ashe, 2001; Games et al., 2006). Consequently, such mice have been studied in an effort to identify toxic Aβ assemblies (Westerman et al., 2002; Kawarabayashi et al., 2004; Lesne et al., 2006; Cheng et al., 2007). The J20 mouse used here expresses APP bearing the Swedish and Indiana mutations, promoting β-secretase cleavage and increasing the $A\beta_{42}/A\beta_{40}$ ratio, respectively (Mucke et al., 2000). These mice show an age-dependent deposition of Aβ beginning around ~4–5 months together with various physiological changes that occur both before (Palop et al., 2007) and after the onset of plaque formation (Palop et al., 2003; Moreno et al., 2007).

Using a sensitive ELISA and a serial extraction procedure to isolate TBS-soluble, triton-soluble and GuHCl-soluble fractions we find that $A\beta_{1–40}$ is the predominant Aβ isoform detected in the aqueous extract, whereas $A\beta_{1–42}$ is the major species detected in the GuHCl extract. Importantly, detection of aggregated Aβ (i.e. Aβ sedimented by centrifugation and subsequently solubilized in GuHCl) preceded immunohistochemical (IHC) detection of amyloid deposits, but at all subsequent intervals the concentration of this GuHCl-solubilized Aβ strongly correlated with the extent of amyloid plaque burden. Assessment of non-fibrillar Aβ assemblies was accomplished using an immunoprecipitation (IP)/Western blot (WB) technique that detects Aβ monomer and SDS-stable low-n oligomers (Walsh et al., 2000; Shankar et al., 2008) and an antioligomer antibody, A11, reported to detect non-fibrillar Aβ oligomers larger than pentamer (Kayed et al., 2003). IHC analysis using the A11 antibody revealed the presence of oligomers at a time coincident with reduced hippocampal MAP2 and synaptophysin immunoreactivity; however, this was evident only at intervals after aggregated Aβ was first detected. Similarly, initial detection of TBS-soluble SDS-stable Aβ dimers occurred several months after the appearance of water-insoluble Aβ aggregates. These findings demonstrate the presence of several different Aβ assemblies in the cerebrum of J20 mice, before, coincident with, and after the onset of detectable synapto-dendritic compromise.

MATERIALS AND METHODS

All chemicals were purchased from Sigma-Aldrich (St. Louis, MO) unless otherwise stated.

Animals and brain collection

The transgenic mouse line, J20, (gift of L. Mucke, Gladstone Institute, UCSF) expresses a human APP minigene with the KM670/671NL and V717F AD-causing mutations driven by a

platelet-derived growth factor promoter (Mucke et al., 2000). J20 mice were maintained on a hybrid background (C57Bl/6 × DBA2) and genotyped by PCR, as described previously (Games et al., 1995; Mucke et al., 2000). Following euthanasia by CO_2 overdose, brains were rapidly removed, placed on an ice-cold glass plate, and bisected sagittally. The left cerebral hemisphere was immediately frozen in liquid nitrogen and stored at −80°C pending biochemical analysis, and the right hemisphere was fixed in 10% formalin for 2 h, dehydrated and embedded in paraffin for sectioning. Animal care and experimental protocols were performed in accordance with applicable portions of the National Institutes of Health Guide for the Care and Use of Laboratory Animals and were approved by Harvard Medical School Institutional Animal Care and Use Committee.

Antibodies

Antibodies to APP and its proteolytic derivatives have been described previously (Walsh et al., 2000). Monoclonal antibody 2G3 was raised to Aβ33–40 and specifically recognizes Aβ species ending at residue 40, whereas monoclonal antibody 21F12 was raised to Aβ33–42 and specifically recognizes Aβ species ending at residue 42 (Johnson-Wood et al., 1997). 3D6 is a monoclonal antibody that specifically recognizes the extreme N-termini of Aβ; 8E5 was raised to a recombinant protein encoding residues 444–592 of APP695 (Games et al., 1995). All four monoclonal antibodies were kindly provided by Drs. P. Seubert and D. Schenk (Elan Pharmaceuticals, South San Francisco, CA). BS42 is a monoclonal antibody highly similar to 21F12 and specifically recognizes Aβ42 and was provided by Dr. David Howlett (GSK, Harlow, Essex, England). R1282 is a high-titer polyclonal antiserum raised to synthetic Aβ1–40 (Haass et al., 1992). Rat anti-mouse CD45 antibody (Serotek Inc., UK) was used to detect microglia while bovine anti-mouse GFAP (1:500; Sigma Immunochemical Co., St. Louis, MO) was used to detect reactive astrocytes. AT8 is a mouse monoclonal antibody that specifically recognizes phosphorylated tau (Innogenetics, Belgium). Anti-synapsin I (AB1543) and anti-synaptophysin antibodies were obtained from Chemicon (Billerica, MA). A11 is a conformation-specific rabbit polyclonal antibody that specifically recognizes Aβ oligomers larger than pentamers (Kayed et al., 2003) and was a gift from Dr. Charles Glabe (University of California, Irvine).

Immunohistochemistry of brain sections

Paraffin-embedded, formalin-fixed 8 μm brain sections were prepared as previously described (Lemere et al., 2002). The Vector Elite horseradish-peroxidase ABC kit (Vector Laboratories Inc., Burlingame, CA) was used with diaminobenzidine (DAB; Sigma Chemical Co., St. Louis, MO), as the chromogen, to visualize immunoreactivity. Plaque-associated immunoreactivity was semi-quantitatively scored as 0 (no staining), 1+ (<10 plaques), 2+ (>10 scattered plaques), 3+ (most of cortex stained), or 4+ (almost confluent staining of cortex and hippocampus).

Preparation of mouse brain homogenates

Whole frozen left hemibrains were cut into small cubes and homogenized using a mechanical dounce homogenizer with 25 strokes in 5 volumes of ice-cold Tris-buffered saline (TBS) containing a cocktail of protease and phosphates inhibitors (0.2 mM Calpeptin, 0.1 mN NaVO3, 50 mM β-gycerolphosphate, 50 mM NaF, 2 mM 1,10 phenanthroline, 5 mM EDTA, 1 mM EGTA, 5 μg/ml leupeptin, 5 μg/ml aprotinin, 2 μg/ml pepstatin, 120 μg/ml Pefabloc, final concentrations). Homogenates were centrifuged in a TLA 100.3 rotar (Beckman, Fulerton, CA) at 175,000 g and 4°C for 30 min. The supernate (designated as the TBS extract) was removed to a clean tube, aliquoted and stored at −80°C. To solubilize Aβ associated with lipids the TBS-insoluble pellet was homogenized (5:1 v:w) in TBS containing 1% Triton X-100 plus inhibitors (TBS-TX) again using 25 strokes of a dounce homogenizer. TBS-TX homogenates were then centrifuged at 175,000 g and 4°C for 30 min and the resultant supernate (i.e. the TBS-TX

extract) was aliquoted and stored at −80°C. In order to release aggregated Aβ not soluble in either TBS or TBS-TX, the TBS-TX pellet was homogenized in 10 volumes of 50 mM Tris-HCl buffer, pH 8.0 containing 5M guanidine HCl and incubated on a Nutator for 14 h at 4°C. Thereafter this suspension, referred to as the GuHCl extract, was aliquoted and stored at −80° C.

For certain experiments cerebral cortex was dissected away from the cerebellum and hindbrain and both hemispheres serially extracts as described above.

Quantification of Aβ in brain extract

Aβ levels in brain extracts were analyzed using a sandwich enzyme-linked immunosorbent assay (ELISA), as described previously (Sun et al., 2002). Briefly, 2G3 and 21F12 were used to capture $A\beta_{40}$ and $A\beta_{42}$, respectively and biotinylated 3D6 was used for detection. TBS and TBS-TX samples that contained high levels of Aβ were diluted with the corresponding blank buffers. In order to neutralize the denaturing activity of 5M GuHCl, all guanidinium-containing extracts were diluted 1:10 in ice-cold casein buffer (0.25% casein, 0.05% sodium azide, 5mM EDTA, 10 ug/ml leupeptin, 10 ug/ml aprotinin in TBS), vortex mixed, centrifuged at 16,000 g and 4°C for 15 min and subsequent dilutions made using 0.5M guanidine, 0.1% BSA in TBS. All samples were analyzed in duplicate and where possible at least two different dilutions of each sample were assayed.

Immunoprecipitation (IP)/Western blot (WB) analysis

A sensitive IP/WB protocol (Walsh et al., 2000) was used for the detection of Aβ in J20 mouse brain extracts. Samples were immunoprecipitated with the high-affinity antibody, R1282, at a dilution of 1:100. TBS and TBS-TX extracts were IP'ed directly and GuHCl extracts were diluted 1:40 in DMEM and then IP'ed. After IP, samples were electrophoresed on either 4–12% polyacrylamide bis-tris or 10–20% polyacrylamide tris-tricine gels (GE Healthcare, Little Chalfont, England) and transferred onto 0.2 μm nitrocellulose membranes at 400 mA for 2 h. Filters were boiled for 10 min in PBS (Ida et al., 1996) and then blocked overnight at 4°C with 5% fat-free milk in 20 mM Tris-HCl, pH 7.4, containing 150 mM NaCl and 0.05% Tween20 (TBS-T). After washing the membranes in TBS-T, they were probed with 2G3 and 21F12 (each at 1 μg/ml). Bound antibody was visualized with horseradish peroxidase conjugated donkey anti-mouse IgG (at 1:25,000) (Jackson ImmunoResearch, West Grove, PA) and the ECL^{+} detection system (GE Healthcare, Little Chalfont, UK) or with the LiCor Odyssey Infrared Imaging System (LI-COR Biosciences, Lincoln, NE) following labeling with IR-dye conjugated to goat anti-mouse (1:5000) (Rockland, Gilbertsville, PA).

Synaptic protein detection

Twenty micrograms of protein from TBS-TX extracts were electrophoresed on 4–12% polyacrylamide bis-tris NuPAGE gels using MOPS running buffer (Invitrogen, Carlsbad, CA). Proteins of interest were visualized on the LiCor Odyssey system following immunoblotting with anti-synapsin I (1 μg/mL), and anti-synaptophysin (1 μg/mL) antibodies and Odyssey software used to determine the relative amount of these synaptic proteins.

Synapse and dendrite quantification

The extent of the synapto-dendritic pathology was determined as previously described (Rockenstein et al., 2005). Blind-coded, 10 μm thick paraffin sections were immunolabeled with mouse monoclonal antibodies against synaptophysin (synaptic marker, 1:20, Chemicon) and microtubule associated protein-2, (MAP2, dendritic marker, 1:40, Chemicon) (Mucke et al., 1995). After overnight incubation with the primary antibodies, sections were incubated with biotin-conjugated horse anti-mouse IgG secondary antibody (1:75, Vector Laboratories),

followed by ABC vector reagent and diaminobendizidine. All sections were processed under the same standardized conditions. The immunolabeled blind-coded sections were serially imaged at 630X with a digital bright field microscope (Olympus) and analyzed based on threshold with the Image Pro-plus as previously described (Toggas et al., 1994; Mucke et al., 1995). For each mouse, four fields in the frontal cortex and hippocampus were examined. All sections were processed simultaneously under the same conditions and experiments were performed twice in order to assess the reproducibility of results. For synaptophysin and MAP2, results are expressed as percent area of the neuropil occupied by immunoreactive terminals and dendrites.

RESULTS

Aβ deposition, A11 immunoreactivity and markers of neuritic dystrophy increase with age in brain of J20 mice

Previous studies of J20 mice have demonstrated that cerebral amyloid deposition begins n 5–7 months old animals (Palop et al., 2003; Cheng et al., 2004). However, given that the extent and onset of plaque formation can be influenced by a variety of factors (Adlard et al., 2005; Lazarov et al., 2005), we systematically characterized the extent of amyloid deposition in a cohort of J20 mice aged between 3–24 months. Immunohistochemical analysis revealed a strong age-dependent increase in amyloid burden and associated neuritic markers (Fig. 1, Table 1). In agreement with prior studies (Mucke et al., 2000; Palop et al., 2003) brains from ~3 month old mice showed no anti-Aβ immunostaining in either the cortex or hippocampus (Table 1). In contrast, all transgenic animals aged between 166 and 171 days (~6 months) had amyloid deposits detectable by R1282 (at least 1 deposits within a 100X field) in both the hippocampus and cortex (Fig. 1a and Table 1), with most animals displaying Aβ42 staining and markers of neuritic pathology (Table 1). Moreover, all J20 mice ~6 months and older exhibited appreciable cortical and hippocampal A11 immunoreactivity. The A11 staining co-localized with R1282 staining of some amyloid plaques, but also included distinct non-plaque staining and increased with age, reaching a plateau between ~12–16 months (Table 1, Fig. 1). The extent of Aβ burden increased proportionately with age, such that by ~16 months most cortical sections from J20 mice were marked by confluent amyloid staining with R1282 (Fig. 1c) and substantial staining with BS42, A11, 8E5 and anti-CD45 (Table 1). We also found that 8 of 17 brains from transgenic mice ~8 months and older had a low, but consistent level of AT8 staining (Table 1). As expected, immunohistochemical analysis of brain sections from non-transgenic mice aged ~3, 16 and 19 months revealed no amyloid deposition and no AT8, 8E5 or anti-CD45 staining and minimal A11 staining (Table 1).

$A\beta_{1-40}$ is the predominant Aβ isoform detected in TBS extracts, whereas $A\beta_{1-42}$ is the major species detected in GuHCl extracts

To complement our immunohistochemical (IHC) analysis we determined the concentration of TBS-soluble, triton-soluble cerebral and GuHCl-extracted Aβ by ELISA. Entire hemi-brains were sequentially extracted first with tris-buffered saline (TBS), then TBS containing 1% Triton X-100 (TBS-TX) and finally 5 M guanidine-HCl (GuHCl). At 3 months, human $A\beta_{1-40}$ was readily detectable in the TBS extract of every J20 animal analyzed, with values ranging between 1.035 – 2.645 ng/g wet weight of brain (Fig. 2a). While the ELISA used here can theoretically detect both endogenous rodent and transgene-derived human Aβ, no appreciable signal was observed in brain homogenates from ~3 month old non-transgenic controls (not shown), thus indicating that the Aβ detected in transgenic mouse brain was predominantly the over-expressed human form. The level of $A\beta_{1-40}$ remained constant until ~12 months at which point there was a slight increase followed by a further increase at ~16 months and a return to ~12 month values at ~19 and 24 months. The content of $A\beta_{1-42}$ in TBS extracts showed a similar trend with barely detectable levels at 3–8 months, increasing at ~12

months, reaching a maximum value at ~16 months and then returning to lower values at ~19 and 24 months. The age-dependent changes in $A\beta_{1–40}$ and $A\beta_{1–42}$ present in the TBS-TX extracts followed a pattern closely similar to that seen in the TBS extracts. Indeed, even the absolute values of Aβ detected were similar for both the TBS and TBS-TX extracts (compare Fig. 2a and b) and in both cases the amount of $A\beta_{1–40}$ exceeded that of $A\beta_{1–42}$ at all time points. Levels of GuHCl-extracted Aβ were at least one order of magnitude higher than TBS or TBS-TX extracted Aβ at all time points greater than 3 months. Even in brains from ~3 month old animals the average concentration of GuHCl-soluble $A\beta_{1–40}$ was ~10 ng/g and this increased dramatically and in a highly age-dependent manner, reaching a maximum value at ~16 months, but remaining constant thereafter (Fig. 2c). Two critical differences between the TBS/TBS-TX and GuHCl extracts were: 1) that after ~3 months $A\beta_{1–42}$ predominated over $A\beta_{1–40}$ in the GuHCl extract and 2) that Aβ levels reached a plateau earlier (~12 months) in the GuHCl fraction and did not fall off thereafter. These results confirm that $A\beta_{1–42}$ is more abundant in amyloid plaques than $A\beta_{1–40}$, but that the latter is the predominant TBS-soluble Aβ species extractable from J20 brain – a pattern we have also observed in Alzheimer brain (J McDonald and DMW, unpublished). Importantly, the $A\beta_{42}$ quantification from the GuHCl extract is consistent with the age-dependent increase in detection of amyloid deposits by BS42 (Table 1). Accordingly, the different representation of Aβ isoforms contained in the TBS soluble and GuHCl-soluble extracts strongly suggest that the Aβ detected in aqueous extracts represent authentic soluble Aβ, not peptides released by partial disruption of $A\beta_{1–42}$-rich amyloid plaques.

ELISA quantified Aβ in GuHCl extracts of brain strongly correlate with amyloid burden visualized by immunohistochemistry

Linear regression analysis comparing R1282 immunoreactivity and ELISA quantitation of extracted Aβ reveal that amyloid deposition strongly co-varies with the Aβ levels in GuHCl extracts (Fig. 3c, R^2=0.93), but correlates less well with TBS-soluble and triton-soluble Aβ species (Figs. 3a, b; R^2=0.69 and 0.77, respectively). Notably, for animals with no (0), low (+1) or moderate (+2) amyloid burden the amounts of Aβ detected in the TBS and TBS-TX extracts were essentially the same, suggesting that TBS-extractable Aβ is not artifactually released from amyloid deposits during homogenization. This is further supported by the prior finding that $A\beta_{40}$ predominates in TBS and TBS-TX extracts, unlike in GuHCl extracts and amyloid deposits (Table 1 and Fig. 2). Furthermore, the marked increase in TBS-extracted Aβ concentration in brains that exhibit higher amyloid deposition (IHC grades 3–4) suggests that the capacity of amyloid plaques to sequester interstitial Aβ in the cortical parenchyma is saturable. This supralinear relationship is best appreciated when TBS-soluble Aβ values are plotted against GuHCl-soluble Aβ (Fig. 3d) and reveals a dramatic increase in TBS-soluble Aβ levels after GuHCl-soluble Aβ reaches ~450 ng/g wet brain weight. A similar relationship is also seen between TBS-TX-soluble Aβ and GuHCl-extracted Aβ (data not shown). These data suggest a dynamic inter-play between highly aggregated plaque Aβ and soluble Aβ, with the $A\beta_{42}$/ $A\beta_{40}$ ratio in TBS and TBS-TX fractions increasing in animals with extensive (+3) and severe (+4) amyloid burden. These results suggest that if an elevated $A\beta_{42}/A\beta_{40}$ ratio is pathogenic it can only exerts its effect via soluble Aβ at a stage when there is already fulment amyloid pathology.

SDS-stable Aβ dimers, trimers and tetramers are detected in J20 brain

Recent data suggests that non-fibrillar soluble oligomeric forms of Aβ are responsible for synaptic compromise (Lambert et al., 1998; Walsh et al., 2002; Lesne et al., 2006; Shankar et al., 2008) and perturbation of learned behavior (Cleary et al., 2005). However, most Aβ ELISAs including the assay used in this study detect monomeric Aβ sensitively, but weakly detect higher Aβ assemblies (Morishima-Kawashima and Ihara, 1998; Stenh et al., 2005). While the ELISA analysis reported above provides useful information about the source of Aβ (i.e.

whether it is derived from soluble or insoluble brain fractions) and whether the species sediment under high speed centrifugation, this method offers no information about the relative amounts of the different assembly forms comprising the total Aβ detected by ELISA. Consequently, we employed 2 different approaches to gain insight into the aggregation state of Aβ present in J20 brain. IHC analysis revealed the presence of A11 (Kayed et al., 2003) positive deposits in the brains of all transgenic animals ~6 months and older (Table 1). A11 immunoreactivity coincided with or preceded BS42 immunostaining, microglial activation and detection of aberrantly phosphorylated tau. Weak IHC staining was also observed in some aged non-transgenic animals; but given that A11 is not specific for oligomers of Aβ alone, it seems likely that this was attributable to oligomers of other misfolded proteins which occur at low levels in aged normal brain tissue. Nonetheless, the higher intensity of A11 immunoreactivity observed in J20 animals suggests that the predominant A11 signal was specific for the expression of the transgene and is indicative of an age-dependent build up of Aβ oligomers.

Similarly, IP/WB analysis of the same cerebral extracts used for ELISA demonstrated an age-dependent appearance of Aβ analogous to that seen in Fig. 2. Using antibodies specific for the extreme C-termini of $A\beta_{1–40/42}$ a faint band migrating around ~4–5 kDa was detected in the TBS extracts of all ~3 month old transgenic mice (Figs. 4a). The specificity of this band was confirmed by the fact that it was not detected in any of the 10 non-transgenic brains examined (Fig. 4a, upper left panel: compare lane 11, ~24 month J20 extract, with lane 12, ~19 month non-transgenic extract) and that it perfectly co-migrated with a synthetic $A\beta_{1–40}$ standard. In agreement with results obtained by ELISA, the level of monomer remained constant between 3–8 months, slightly increased at ~12 months and reached a maximum at ~16 months. No other specific bands were detected in brain extracts of J20 animals aged 3–8 months; however, in one of the five month old J20s (not shown) and in all of the ten J20s ~16 month and older an additional band migrating ~7–8 kDa was detected. As with the monomer, this SDS-stable dimer was not detected in any of the non-transgenic brains studied, and no additional higher molecular weight bands specific to J20 mouse brain were detected. A similar pattern was also seen in TBS-TX and GuHCl extracts. Notably, the amount of Aβ present in the GuHCl extract was considerably higher than either the TBS or TBS-TX extracts, such that only ~$1/7^{th}$ of GuHCl extract was required to achieve a similar signal intensity as achieved with TBS or TBS-TX extracts. Thus, in agreement with the ELISA results the amount of Aβ extracted with GuHCl is approximately 1 order of magnitude higher than the amount of aqueous- or detergent-soluble Aβ. Additionally, insoluble Aβ was discernable in some animals as early ~3 months (Fig. 4c).

To assess whether dimers are present at earlier ages, four times the amount of GuHCl extract used in Fig. 4c was IP'ed. Analysis of this larger amount of starting material allowed for the visualization of dimers beginning at ~6–8 months (Figs. 4d, e) and at later time points specific bands migrating ~12 and ~16 kDa (putative trimers and tetramers) were detected. Clearly the ability to detect SDS-stable low-n oligomers in the GuHCl extract was dependent upon the amount of material used, thus raising the possibility that dimers, trimer and tetramers may be present at earlier time points and in other fractions, but are below the level of detection under the conditions used. While it was possible to use larger volumes of GuHCl brain extracts to search for SDS-stable low-n oligomers (Fig. 4d), unfortunately it was not possible to analyze large volumes of TBS or TBS-TX extracts since all of this material had been consumed for other assays.

Measures of total cerebral synaptic integrity fail to show age- and genotype-dependent changes in the face of reduced hippocampal MAP2 and synaptophysin immunoreactivity

We also sought to determine if temporal changes in the solubility and assembly forms of Aβ correlate with pathologically relevant changes in synaptic markers. To do this we again employed biochemical and IHC approaches. Using the same brain extracts from which Aβ

levels were measured we assessed the levels of the pre-synaptic markers synaptophysin and synapsin. No significant differences were observed in the levels of these proteins when comparing samples from J20 and non-transgenic animals (Fig. 5a). For instance, densitometric analysis in extracts from 19 month old J20 mice across 3 experiments revealed that the amount of synaptophysin was 109±15% of that detected in extracts from aged matched non-tg brains and the level of synapsin was 95±10% of controls. Because this analysis was performed on extracts from the entire cerebrum, these results suggest that widespread synaptic compromise is not a feature of this mouse model. Therefore we investigated if regional specific synapse loss was detectable. Subsequent analysis of the hippocampus, a region that displays significant synapse loss in AD, revealed transgene-specific effects, with a significant decrease in synaptophysin density in J20 mice compared to non-transgenic mice evident by ~6–8 months (Fig. 5c,d 22.7±0.6% vs. 27.6±0.5%, respectively, $p<0.05$). Similarly, MAP2 staining also demonstrated decreases in J20 mice by this age (Fig. 5b,d 21.6±0.7% vs. 26.8±0.7%, respectively, $p<0.05$), suggesting dendritic loss in hippocampus. Both of these differences maintained significance at ~16–19 months.

DISCUSSION

The amyloid cascade hypothesis of Alzheimer's disease posits that disruption of normal brain Aβ metabolism initiates a chain of events that ultimately causes disease (Hardy and Allsop, 1991; Selkoe, 1991; Klein et al., 2001; Hardy and Selkoe, 2002). This hypothesis is supported by extensive genetic, biochemical and animal modeling, yet the hypothesis remains controversial because amyloid histopathology does not correlate well with disease (Terry et al., 1991). The steady state level of Aβ is controlled by production, degradation and clearance; at micromolar concentrations Aβ can self-associate forming a variety of different assemblies: ranging from dimers to aggregates of amyloid fibrils (for review see: (Walsh and Selkoe, 2007). However, as yet the specific form(s) of Aβ which causes injury to neurons *in vivo* has not been identified. In recent years biochemical analysis of AD brain revealed a robust correlation between soluble Aβ levels and the extent of synaptic loss and severity of cognitive impairment (McLean et al., 1999; Lemere et al., 2002; Atwood et al., 2004). In such studies water-soluble Aβ is defined by two properties: 1) that it is released by homogenization in an aqueous buffer and therefore is likely to be derived from both the interstitial fluid of the parenchyma and from the cytosol, and 2) it does not readily sediment and therefore is unlikely to contain large particulates such as amyloid plaques or meshworks of amyloid fibrils. Typically, measurement of soluble Aβ has been achieved using assays that cannot identify the aggregation state of the species detected and may under-report the true level of Aβ oligomers (Funato et al., 1998; Morishima-Kawashima and Ihara, 1998; Stenh et al., 2005). Thus, although the assembly states of these Aβ species are unknown, their failure to pellet following ultracentrifugation indicates that they are not fibrillar in nature, but attempts to further characterize these species have been limited.

Further evidence supporting soluble forms of Aβ as the principal mediators of neuronal compromise comes from studies of APP transgenic mice reporting alterations in neuronal morphology and physiology observed well before the first signs of amyloid deposition (Chapman et al., 1999; Hsia et al., 1999; Moechars et al., 1999; Mucke et al., 2000; Dineley et al., 2002; Westerman et al., 2002; Wu et al., 2004) and from studies in which Aβ-mediated deficits of memory were reversed by a single intraperitoneal injection of an anti-Aβ antibody (Dodart et al., 2002). In these acute (<24 hr) experiments, brain amyloid burden was not decreased, suggesting that the antibody was acting on soluble Aβ by neutralizing or clearing these small assemblies.

APP transgenic mice are particularly attractive models for studying Aβ toxicity since they offer the possibility of examining different stages of the "disease process", such that a particular

Aβ assembly may be correlated with the emergence of a certain AD-relevant phenotype (Lesne et al., 2006). In this study we performed extensive biochemical and IHC analyses to better understand the Aβ species present in J20 mouse brain before and after the deposition of detectable plaques or the appearance of disease relevant changes. As reported previously, detectable amyloid deposition began in mice at ~6 months (Mukherjee et al., 2000; Palop et al., 2003). Using IHC and biochemical approaches we searched for evidence of neuritic dystrophy and signs of synaptic compromise. As with recent findings (Palop et al., 2007) we found no evidence of global synaptic loss; however, analysis of the hippocampus, a region that displays synapse loss in AD, revealed a significant decrease in both synaptophysin and MAP2 immunoreactivity. These data support a model for selective vulnerability of certain classes of neurons to Aβ (Capetillo-Zarate et al., 2006; Palop et al., 2007). Furthermore, although significance was not reached at 3 months, there was a stronger trend towards decreased synaptophysin than MAP2 staining, suggesting that synapse pruning likely occurs prior to dendritic loss. The results described here also revealed a supralinear relationship between soluble and insoluble Aβ after a certain threshold of amyloid deposition is reached, suggesting an explanation for why AD manifests in the aging brain. These data imply that the cerebral parenchyma may have a limited capacity to sequester soluble forms of Aβ. After this level has been exceeded, synapse and neuronal degeneration manifests and accelerates in cortex that is faced with an increasing soluble Aβ oligomer burden. This hypothesis is further supported by previous findings that amyloid plaques do not increase in size or number in the already aged brain (Hyman et al., 1995; Lemere et al., 1996).

These data, however, do not elucidate which form(s) of Aβ mediate these synaptic and dendritic changes. For instance, changes in synaptophysin and MAP2 only become statistically significant at ~6 month, despite the earlier presence of aggregated Aβ. Moreover, biochemical fractionation coupled with ELISA revealed that even at the earliest time intervals studied, the brains of all J20 mice contained aggregated forms of Aβ insoluble in TBS and TBS-TX and pelleted by high speed centrifugation. At ages when plaques were evident, the amount of Aβ extracted in GuHCl strongly correlated with amyloid burden, indicating that the GuHCl fraction likely represents plaque-associated Aβ. If indeed this is the case, the detection of Aβ in this fraction at ~3 months suggests that tiny insoluble amyloid aggregates are present, but are too small to be visualized by light microscopy. By ~6 months appreciable A11 immunoreactivity was evident, some of which was associated with plaques and some of which appeared to be completely independent of plaques. We also determined that J20 mouse brain contains SDS-stable low-n Aβ oligomers, such as those detected in human CSF, aqueous brain extracts and in medium from certain cultured cells, and which can impair synaptic plasticity and the memory of learned behavior (Walsh et al., 2002; Klyubin et al., 2008; Shankar et al., 2008). Consistent with our ELISA results the monomer was evident in all brain fractions from the earliest age studied. In contrast Aβ dimer was only routinely detected in TBS extracts from animals 12 months and older and this was also true for the TBS-TX and GuHCl extracts. Thus, from these results it would appear that SDS-stable Aβ dimers appear several months after the onset of synaptodendritic loss. Of course the lack of detection of a certain species does not preclude the involvement of that species in pathology, since it may be present and active, but at concentrations below the detection limit of the assay. In this study, SDS-stable dimers were observable as early as 6 months when a larger volume of GuHCl sample was analyzed, suggesting that the detection of a given Aβ species depends on the amount of tissue extract analyzed. Furthermore, this larger volume of analysate also permitted the visualization of larger Aβ assemblies, namely trimers and tetramers, the detection of which coincided with the rapid accumulation of plaques that occurs around 12 months. The presence of such species could either indicate the increased presence of SDS-stable oligomers in plaques or more likely the incomplete denaturation of Aβ fibrils.

This lack of coincident detection of a particular synaptotoxic species and the appearance of a given phenotype does not necessarily exclude the involvement of that species in the observed phenotype. For instance, Lesne and colleagues reported that in brain extracts from Tg2576 mice ~42 kDa (nonamer) and ~56 kDa (dodecamer) Aβ species were detected at an age that coincided with the first observed changes in spatial memory (Lesne et al., 2006). However, Kawarabayashi and colleagues reported that the appearance of SDS-stable dimers present in lipid rafts also coincided with impairment of spatial memory (Kawarabayashi et al., 2004). Similarly, it has been documented that the same Tg2576 mice show impaired performance in a hippocampal-dependent contextual fear conditioning assay, decreased spine density in the dentate gyrus, and impairment of long term potentiation (LTP) at ages long before the first detection of Aβ dodecamer (Dineley et al., 2002; Jacobsen et al., 2006; Lesne et al., 2006). Thus, while the appearance of dodecamers correlates with the impairment of spatial memory in Tg2576 mice, it does not correlate with changes in other forms of memory, nor do dodecamer levels correlate with changes in synaptic form and function. Indeed, the results presented here suggest that synaptotoxicity is mediated by multiple Aβ species; therefore, coincidence of detection of a specific assembly and effect on neuronal physiology alone are insufficient to define the active species. Other very recent data also support the presence of multiple bioactive Aβ species in J20 mouse brain (Meilandt et al., 2009). Over-expression of neprilysin dramatically reduced total Aβ levels, but did not alter Aβ56* and SDS-stable Aβ trimer levels nor did it recover spatial reference learning and memory impairments evident in J20 mice. In addition, changes in hippocampal Fos levels and hyperactivity were attributed to a third unidentified species (Meilandt et al., 2009). How the species detected by Meilandt and colleagues relates to those forms of Aβ detected in this study is uncertain, since the authors did not quantify either the presence of A11 immunoreactive species or the level of water and triton X100-insoluble species.

Similarly, while substantial data, particularly from the study of familial AD mutations, support a central pathogenic role for Aβ42 (Klein et al., 2001), synaptotoxicity cannot simply be ascribed to a single Aβ primary sequence. Not least since we have recently demonstrated that TBS extracts of AD brain rich in Aβ40 can alter synaptic form and function and impair memory consolidation (Shankar et al., 2008). Thus this study of J20 brain demonstrates the presence of multiple Aβ species differing in solubility and aggregation state, suggesting that the various neuronal impairments documented in these mice likely result from the activity of more than one Aβ assembly form. These data are also consistent with the situation found in human brain were water-soluble, detergent-soluble and formic acid-soluble Aβ species have also been found to co-exist (Lue et al., 1999; McLean et al., 1999; Wang et al., 1999). With the water-soluble phase of AD brain containing a broad spectrum of Aβ assemblies ranging from monomer to species with molecular weights ≥100 kDa (Kuo et al., 1996).

Acknowledgments

We thank Dr. Lennart Mucke (UCSF) for the gift of J20 founders and Drs. P. Seubert, D. Schenk (Elan Pharmaceuticals, South San Francisco, CA) and D. Howlett (GSK, Harlow, England) for antibodies. We are also grateful to Ms. Julia Fadeeva for technical assistance. This work was supported by Wellcome Trust grant 067660 (DMW) and National Institute on Aging Grants 1R01AG027443 (DMW and DJS), AG18440, AG022074, AG10435 (EM) and AG20159 (CL). GMS was the recipient of an EU Marie-Curie short-term fellowship.

REFERENCES

Pathological correlates of late-onset dementia in a multicentre, community-based population in England and Wales. Neuropathology Group of the Medical Research Council Cognitive Function and Ageing Study (MRC CFAS). Lancet 2001;357:169–175. [PubMed: 11213093]

Adlard PA, Perreau VM, Pop V, Cotman CW. Voluntary exercise decreases amyloid load in a transgenic model of Alzheimer's disease. J Neurosci 2005;25:4217–4221. [PubMed: 15858047]

Ashe KH. Learning and memory in transgenic mice modeling Alzheimer's disease. Learn Mem 2001;8:301–308. [PubMed: 11773429]

Atwood CS, Perry G, Zeng H, Kato Y, Jones WD, Ling KQ, Huang X, Moir RD, Wang D, Sayre LM, Smith MA, Chen SG, Bush AI. Copper mediates dityrosine cross-linking of Alzheimer's amyloid-beta. Biochemistry 2004;43:560–568. [PubMed: 14717612]

Bennett DA, Schneider JA, Arvanitakis Z, Kelly JF, Aggarwal NT, Shah RC, Wilson RS. Neuropathology of older persons without cognitive impairment from two community-based studies. Neurology 2006;66:1837–1844. [PubMed: 16801647]

Braak H, Braak E. Frequency of stages of Alzheimer-related lesions in different age categories. Neurobiol Aging 1997;18:351–357. [PubMed: 9330961]

Capetillo-Zarate E, Staufenbiel M, Abramowski D, Haass C, Escher A, Stadelmann C, Yamaguchi H, Wiestler OD, Thal DR. Selective vulnerability of different types of commissural neurons for amyloid beta-protein-induced neurodegeneration in APP23 mice correlates with dendritic tree morphology. Brain 2006;129:2992–3005. [PubMed: 16844716]

Chapman PF, White GL, Jones MW, Cooper-Blacketer D, Marshall VJ, Irizarry M, Younkin L, Good MA, Bliss TV, Hyman BT, Younkin SG, Hsiao KK. Impaired synaptic plasticity and learning in aged amyloid precursor protein transgenic mice. Nat Neurosci 1999;2:271–276. [PubMed: 10195221]

Cheng IH, Palop JJ, Esposito LA, Bien-Ly N, Yan F, Mucke L. Aggressive amyloidosis in mice expressing human amyloid peptides with the Arctic mutation. Nat Med 2004;10:1190–1192. [PubMed: 15502844]

Cheng IH, Scearce-Levie K, Legleiter J, Palop JJ, Gerstein H, Bien-Ly N, Puolivali J, Lesne S, Ashe KH, Muchowski PJ, Mucke L. Accelerating amyloid-beta fibrillization reduces oligomer levels and functional deficits in Alzheimer disease mouse models. J Biol Chem 2007;282:23818–23828. [PubMed: 17548355]

Cleary JP, Walsh DM, Hofmeister JJ, Shankar GM, Kuskowski MA, Selkoe DJ, Ashe KH. Natural oligomers of the amyloid-beta protein specifically disrupt cognitive function. Nat Neurosci 2005;8:79–84. [PubMed: 15608634]

Dickson DW. The pathogenesis of senile plaques. J Neuropathol Exp Neurol 1997;56:321–339. [PubMed: 9100663]

Dineley KT, Xia X, Bui D, Sweatt JD, Zheng H. Accelerated plaque accumulation, associative learning deficits, and up-regulation of alpha 7 nicotinic receptor protein in transgenic mice co-expressing mutant human presenilin 1 and amyloid precursor proteins. J Biol Chem 2002;277:22768–22780. [PubMed: 11912199]

Dodart JC, Bales KR, Gannon KS, Greene SJ, DeMattos RB, Mathis C, DeLong CA, Wu S, Wu X, Holtzman DM, Paul SM. Immunization reverses memory deficits without reducing brain Abeta burden in Alzheimer's disease model. Nat Neurosci 2002;5:452–457. [PubMed: 11941374]

Funato H, Yoshimura M, Kusui K, Tamaoka A, Ishikawa K, Ohkoshi N, Namekata K, Okeda R, Ihara Y. Quantitation of amyloid beta-protein (A beta) in the cortex during aging and in Alzheimer's disease. Am J Pathol 1998;152:1633–1640. [PubMed: 9626067]

Games D, Buttini M, Kobayashi D, Schenk D, Seubert P. Mice as models: transgenic approaches and Alzheimer's disease. J Alzheimers Dis 2006;9:133–149. [PubMed: 16914852]

Games D, Adams D, Alessandrini R, Barbour R, Berthelette P, Blackwell C, Carr T, Clemens J, Donaldson T, Gillespie F, et al. Alzheimer-type neuropathology in transgenic mice overexpressing V717F beta-amyloid precursor protein. Nature 1995;373:523–527. [PubMed: 7845465]

Haass C, Schlossmacher MG, Hung AY, Vigo-Pelfrey C, Mellon A, Ostaszewski BL, Lieberburg I, Koo EH, Schenk D, Teplow DB, et al. Amyloid beta-peptide is produced by cultured cells during normal metabolism. Nature 1992;359:322–325. [PubMed: 1383826]

Hardy J, Allsop D. Amyloid deposition as the central event in the aetiology of Alzheimer's disease. Trends Pharmacol Sci 1991;12:383–388. [PubMed: 1763432]

Hardy J, Selkoe DJ. The amyloid hypothesis of Alzheimer's disease: progress and problems on the road to therapeutics. Science 2002;297:353–356. [PubMed: 12130773]

Hartley DM, Walsh DM, Ye CP, Diehl T, Vasquez S, Vassilev PM, Teplow DB, Selkoe DJ. Protofibrillar intermediates of amyloid beta-protein induce acute electrophysiological changes and progressive neurotoxicity in cortical neurons. J Neurosci 1999;19:8876–8884. [PubMed: 10516307]

Hsia AY, Masliah E, McConlogue L, Yu GQ, Tatsuno G, Hu K, Kholodenko D, Malenka RC, Nicoll RA, Mucke L. Plaque-independent disruption of neural circuits in Alzheimer's disease mouse models. Proc Natl Acad Sci U S A 1999;96:3228–3233. [PubMed: 10077666]

Hyman BT, West HL, Rebeck GW, Buldyrev SV, Mantegna RN, Ukleja M, Havlin S, Stanley HE. Quantitative analysis of senile plaques in Alzheimer disease: observation of log-normal size distribution and molecular epidemiology of differences associated with apolipoprotein E genotype and trisomy 21 (Down syndrome). Proc Natl Acad Sci U S A 1995;92:3586–3590. [PubMed: 7724603]

Ida N, Hartmann T, Pantel J, Schroder J, Zerfass R, Forstl H, Sandbrink R, Masters CL, Beyreuther K. Analysis of heterogeneous A4 peptides in human cerebrospinal fluid and blood by a newly developed sensitive Western blot assay. J Biol Chem 1996;271:22908–22914. [PubMed: 8798471]

Jacobsen JS, Wu CC, Redwine JM, Comery TA, Arias R, Bowlby M, Martone R, Morrison JH, Pangalos MN, Reinhart PH, Bloom FE. Early-onset behavioral and synaptic deficits in a mouse model of Alzheimer's disease. Proc Natl Acad Sci U S A 2006;103:5161–5166. [PubMed: 16549764]

Johnson-Wood K, Lee M, Motter R, Hu K, Gordon G, Barbour R, Khan K, Gordon M, Tan H, Games D, Lieberburg I, Schenk D, Seubert P, McConlogue L. Amyloid precursor protein processing and A beta42 deposition in a transgenic mouse model of Alzheimer disease. Proc Natl Acad Sci U S A 1997;94:1550–1555. [PubMed: 9037091]

Kawarabayashi T, Shoji M, Younkin LH, Wen-Lang L, Dickson DW, Murakami T, Matsubara E, Abe K, Ashe KH, Younkin SG. Dimeric amyloid beta protein rapidly accumulates in lipid rafts followed by apolipoprotein E and phosphorylated tau accumulation in the Tg2576 mouse model of Alzheimer's disease. J Neurosci 2004;24:3801–3809. [PubMed: 15084661]

Kayed R, Head E, Thompson JL, McIntire TM, Milton SC, Cotman CW, Glabe CG. Common structure of soluble amyloid oligomers implies common mechanism of pathogenesis. Science 2003;300:486–489. [PubMed: 12702875]

Klein WL, Krafft GA, Finch CE. Targeting small Abeta oligomers: the solution to an Alzheimer's disease conundrum? Trends Neurosci 2001;24:219–224. [PubMed: 11250006]

Klyubin I, Walsh DM, Cullen WK, Fadeeva JV, Anwyl R, Selkoe DJ, Rowan MJ. Soluble Arctic amyloid beta protein inhibits hippocampal long-term potentiation in vivo. Eur J Neurosci 2004;19:2839–2846. [PubMed: 15147317]

Klyubin I, Betts V, Welzel AT, Blennow K, Zetterberg H, Wallin A, Lemere CA, Cullen WK, Peng Y, Wisniewski T, Selkoe DJ, Anwyl R, Walsh DM, Rowan MJ. Amyloid beta protein dimer-containing human CSF disrupts synaptic plasticity: prevention by systemic passive immunization. J Neurosci 2008;28:4231–4237. [PubMed: 18417702]

Kuo YM, Emmerling MR, Vigo-Pelfrey C, Kasunic TC, Kirkpatrick JB, Murdoch GH, Ball MJ, Roher AE. Water-soluble Abeta (N-40, N-42) oligomers in normal and Alzheimer disease brains. J Biol Chem 1996;271:4077–4081. [PubMed: 8626743]

Lacor PN, Buniel MC, Furlow PW, Clemente AS, Velasco PT, Wood M, Viola KL, Klein WL. Abeta oligomer-induced aberrations in synapse composition, shape, and density provide a molecular basis for loss of connectivity in Alzheimer's disease. J Neurosci 2007;27:796–807. [PubMed: 17251419]

Lambert MP, Barlow AK, Chromy BA, Edwards C, Freed R, Liosatos M, Morgan TE, Rozovsky I, Trommer B, Viola KL, Wals P, Zhang C, Finch CE, Krafft GA, Klein WL. Diffusible, nonfibrillar ligands derived from Abeta1-42 are potent central nervous system neurotoxins. Proc Natl Acad Sci U S A 1998;95:6448–6453. [PubMed: 9600986]

Lazarov O, Robinson J, Tang YP, Hairston IS, Korade-Mirnics Z, Lee VM, Hersh LB, Sapolsky RM, Mirnics K, Sisodia SS. Environmental enrichment reduces Abeta levels and amyloid deposition in transgenic mice. Cell 2005;120:701–713. [PubMed: 15766532]

Lemere CA, Spooner ET, Leverone JF, Mori C, Clements JD. Intranasal immunotherapy for the treatment of Alzheimer's disease: Escherichia coli LT and LT(R192G) as mucosal adjuvants. Neurobiol Aging 2002;23:991–1000. [PubMed: 12470794]

Lemere CA, Blusztajn JK, Yamaguchi H, Wisniewski T, Saido TC, Selkoe DJ. Sequence of deposition of heterogeneous amyloid beta-peptides and APO E in Down syndrome: implications for initial events in amyloid plaque formation. Neurobiol Dis 1996;3:16–32. [PubMed: 9173910]

Lesne S, Koh MT, Kotilinek L, Kayed R, Glabe CG, Yang A, Gallagher M, Ashe KH. A specific amyloid-beta protein assembly in the brain impairs memory. Nature 2006;440:352–357. [PubMed: 16541076]

Lue LF, Kuo YM, Roher AE, Brachova L, Shen Y, Sue L, Beach T, Kurth JH, Rydel RE, Rogers J. Soluble amyloid beta peptide concentration as a predictor of synaptic change in Alzheimer's disease. Am J Pathol 1999;155:853–862. [PubMed: 10487842]

McLean CA, Cherny RA, Fraser FW, Fuller SJ, Smith MJ, Beyreuther K, Bush AI, Masters CL. Soluble pool of Abeta amyloid as a determinant of severity of neurodegeneration in Alzheimer's disease. Ann Neurol 1999;46:860–866. [PubMed: 10589538]

Meilandt WJ, Cisse M, Ho K, Wu T, Esposito LA, Scearce-Levie K, Cheng IH, Yu GQ, Mucke L. Neprilysin overexpression inhibits plaque formation but fails to reduce pathogenic Abeta oligomers and associated cognitive deficits in human amyloid precursor protein transgenic mice. J Neurosci 2009;29:1977–1986. [PubMed: 19228952]

Mirra SS, Heyman A, McKeel D, Sumi SM, Crain BJ, Brownlee LM, Vogel FS, Hughes JP, van Belle G, Berg L. The Consortium to Establish a Registry for Alzheimer's Disease (CERAD). Part II. Standardization of the neuropathologic assessment of Alzheimer's disease. Neurology 1991;41:479–486. [PubMed: 2011243]

Moechars D, Dewachter I, Lorent K, Reverse D, Baekelandt V, Naidu A, Tesseur I, Spittaels K, Haute CV, Checler F, Godaux E, Cordell B, Van Leuven F. Early phenotypic changes in transgenic mice that overexpress different mutants of amyloid precursor protein in brain. J Biol Chem 1999;274:6483–6492. [PubMed: 10037741]

Moreno H, Wu WE, Lee T, Brickman A, Mayeux R, Brown TR, Small SA. Imaging the Abeta-related neurotoxicity of Alzheimer disease. Arch Neurol 2007;64:1467–1477. [PubMed: 17923630]

Morishima-Kawashima M, Ihara Y. The presence of amyloid beta-protein in the detergent-insoluble membrane compartment of human neuroblastoma cells. Biochemistry 1998;37:15247–15253. [PubMed: 9799484]

Mucke L, Abraham CR, Ruppe MD, Rockenstein EM, Toggas SM, Mallory M, Alford M, Masliah E. Protection against HIV-1 gp120-induced brain damage by neuronal expression of human amyloid precursor protein. J Exp Med 1995;181:1551–1556. [PubMed: 7699335]

Mucke L, Masliah E, Yu GQ, Mallory M, Rockenstein EM, Tatsuno G, Hu K, Kholodenko D, Johnson-Wood K, McConlogue L. High-level neuronal expression of abeta 1–42 in wild-type human amyloid protein precursor transgenic mice: synaptotoxicity without plaque formation. J Neurosci 2000;20:4050–4058. [PubMed: 10818140]

Mukherjee A, Song E, Kihiko-Ehmann M, Goodman JP Jr, Pyrek JS, Estus S, Hersh LB. Insulysin hydrolyzes amyloid beta peptides to products that are neither neurotoxic nor deposit on amyloid plaques. J Neurosci 2000;20:8745–8749. [PubMed: 11102481]

Palop JJ, Jones B, Kekonius L, Chin J, Yu GQ, Raber J, Masliah E, Mucke L. Neuronal depletion of calcium-dependent proteins in the dentate gyrus is tightly linked to Alzheimer's disease-related cognitive deficits. Proc Natl Acad Sci U S A 2003;100:9572–9577. [PubMed: 12881482]

Palop JJ, Chin J, Roberson ED, Wang J, Thwin MT, Bien-Ly N, Yoo J, Ho KO, Yu GQ, Kreitzer A, Finkbeiner S, Noebels JL, Mucke L. Aberrant excitatory neuronal activity and compensatory remodeling of inhibitory hippocampal circuits in mouse models of Alzheimer's disease. Neuron 2007;55:697–711. [PubMed: 17785178]

Puzzo D, Privitera L, Leznik E, Fa M, Staniszewski A, Palmeri A, Arancio O. Picomolar amyloid-beta positively modulates synaptic plasticity and memory in hippocampus. J Neurosci 2008;28:14537–14545. [PubMed: 19118188]

Rockenstein E, Mante M, Alford M, Adame A, Crews L, Hashimoto M, Esposito L, Mucke L, Masliah E. High beta-secretase activity elicits neurodegeneration in transgenic mice despite reductions in amyloid-beta levels: implications for the treatment of Alzheimer disease. J Biol Chem 2005;280:32957–32967. [PubMed: 16027115]

Schonheit B, Zarski R, Ohm TG. Spatial and temporal relationships between plaques and tangles in Alzheimer-pathology. Neurobiol Aging 2004;25:697–711. [PubMed: 15165691]

Selkoe DJ. The molecular pathology of Alzheimer's disease. Neuron 1991;6:487–498. [PubMed: 1673054]

Selkoe DJ. Alzheimer's disease: genes, proteins, and therapy. Physiol Rev 2001;81:741–766. [PubMed: 11274343]

Shankar GM, Li S, Mehta TH, Garcia-Munoz A, Shepardson NE, Smith I, Brett FM, Farrell MA, Rowan MJ, Lemere CA, Regan CM, Walsh DM, Sabatini BL, Selkoe DJ. Amyloid-beta protein dimers isolated directly from Alzheimer's brains impair synaptic plasticity and memory. Nat Med 2008;14:837–842. [PubMed: 18568035]

Stenh C, Englund H, Lord A, Johansson AS, Almeida CG, Gellerfors P, Greengard P, Gouras GK, Lannfelt L, Nilsson LN. Amyloid-beta oligomers are inefficiently measured by enzyme-linked immunosorbent assay. Ann Neurol 2005;58:147–150. [PubMed: 15984012]

Sun X, Sato S, Murayama O, Murayama M, Park JM, Yamaguchi H, Takashima A. Lithium inhibits amyloid secretion in COS7 cells transfected with amyloid precursor protein C100. Neurosci Lett 2002;321:61–64. [PubMed: 11872257]

Terry RD, Hansen LA, DeTeresa R, Davies P, Tobias H, Katzman R. Senile dementia of the Alzheimer type without neocortical neurofibrillary tangles. J Neuropathol Exp Neurol 1987;46:262–268. [PubMed: 2881985]

Terry RD, Masliah E, Salmon DP, Butters N, DeTeresa R, Hill R, Hansen LA, Katzman R. Physical basis of cognitive alterations in Alzheimer's disease: synapse loss is the major correlate of cognitive impairment. Ann Neurol 1991;30:572–580. [PubMed: 1789684]

Toggas SM, Masliah E, Rockenstein EM, Rall GF, Abraham CR, Mucke L. Central nervous system damage produced by expression of the HIV-1 coat protein gp120 in transgenic mice. Nature 1994;367:188–193. [PubMed: 8114918]

Walsh DM, Selkoe DJ. A beta oligomers - a decade of discovery. J Neurochem 2007;101:1172–1184. [PubMed: 17286590]

Walsh DM, Tseng BP, Rydel RE, Podlisny MB, Selkoe DJ. The oligomerization of amyloid beta-protein begins intracellularly in cells derived from human brain. Biochemistry 2000;39:10831–10839. [PubMed: 10978169]

Walsh DM, Klyubin I, Fadeeva JV, Cullen WK, Anwyl R, Wolfe MS, Rowan MJ, Selkoe DJ. Naturally secreted oligomers of amyloid beta protein potently inhibit hippocampal long-term potentiation in vivo. Nature 2002;416:535–539. [PubMed: 11932745]

Wang HW, Pasternak JF, Kuo H, Ristic H, Lambert MP, Chromy B, Viola KL, Klein WL, Stine WB, Krafft GA, Trommer BL. Soluble oligomers of beta amyloid (1–42) inhibit long-term potentiation but not long-term depression in rat dentate gyrus. Brain Res 2002;924:133–140. [PubMed: 11750898]

Wang J, Dickson DW, Trojanowski JQ, Lee VM. The levels of soluble versus insoluble brain Abeta distinguish Alzheimer's disease from normal and pathologic aging. Exp Neurol 1999;158:328–337. [PubMed: 10415140]

Wang Q, Walsh DM, Rowan MJ, Selkoe DJ, Anwyl R. Block of long-term potentiation by naturally secreted and synthetic amyloid beta-peptide in hippocampal slices is mediated via activation of the kinases c-Jun N-terminal kinase, cyclin-dependent kinase 5, and p38 mitogen-activated protein kinase as well as metabotropic glutamate receptor type 5. J Neurosci 2004;24:3370–3378. [PubMed: 15056716]

Westerman MA, Cooper-Blacketer D, Mariash A, Kotilinek L, Kawarabayashi T, Younkin LH, Carlson GA, Younkin SG, Ashe KH. The relationship between Abeta and memory in the Tg2576 mouse model of Alzheimer's disease. J Neurosci 2002;22:1858–1867. [PubMed: 11880515]

Wu CC, Chawla F, Games D, Rydel RE, Freedman S, Schenk D, Young WG, Morrison JH, Bloom FE. Selective vulnerability of dentate granule cells prior to amyloid deposition in PDAPP mice: digital morphometric analyses. Proc Natl Acad Sci U S A 2004;101:7141–7146. [PubMed: 15118092]

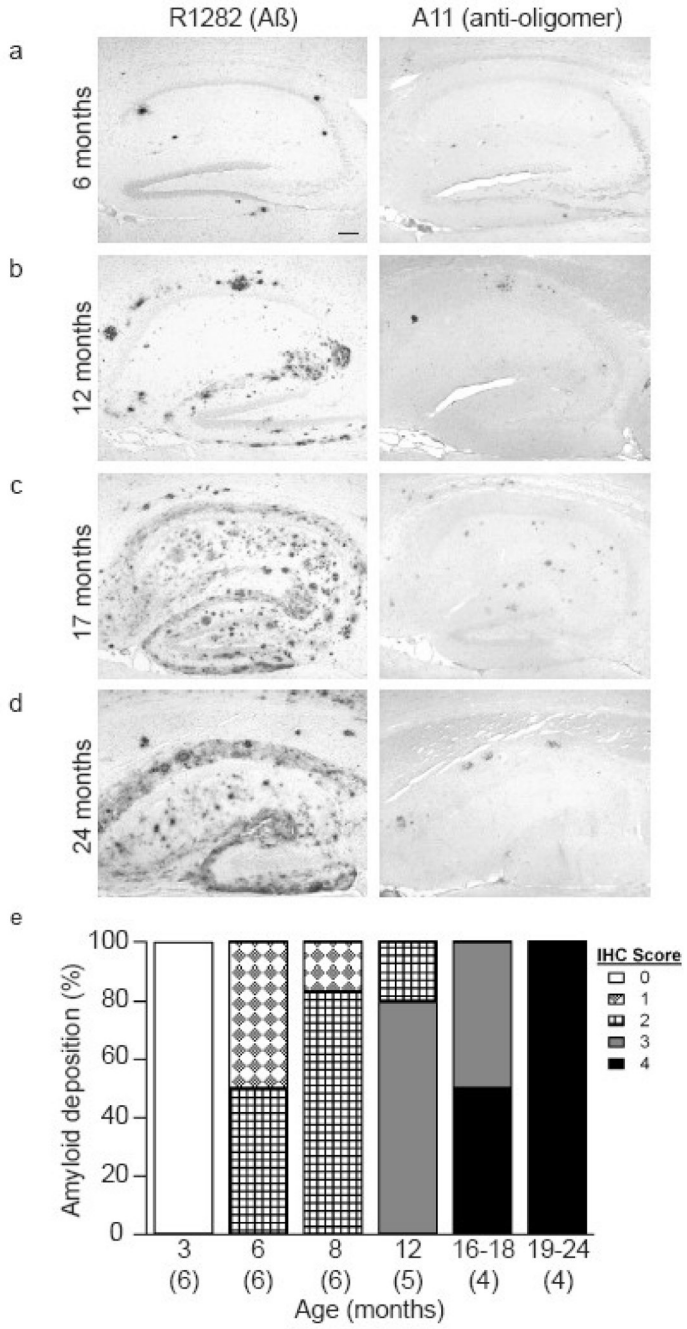

Figure 1. J20 mice display an age-dependent increase in amyloid deposition

Brain sections from J20 mice of approximately (a) 6, (b) 12, (c) 17, and (d) 24 months were immunostained with the polyclonal anti-Aβ antibody R1282 (left) or Aβ oligomer-specific antibody A11 (right). Scale bar on the left panel of (a) is 100 μm. (e) The extent of amyloid deposition detectable with R1282 at 3, 6, 8, 12 and 19–24 months is represented graphically, with the number of mice in each group indicated in parenthesis.

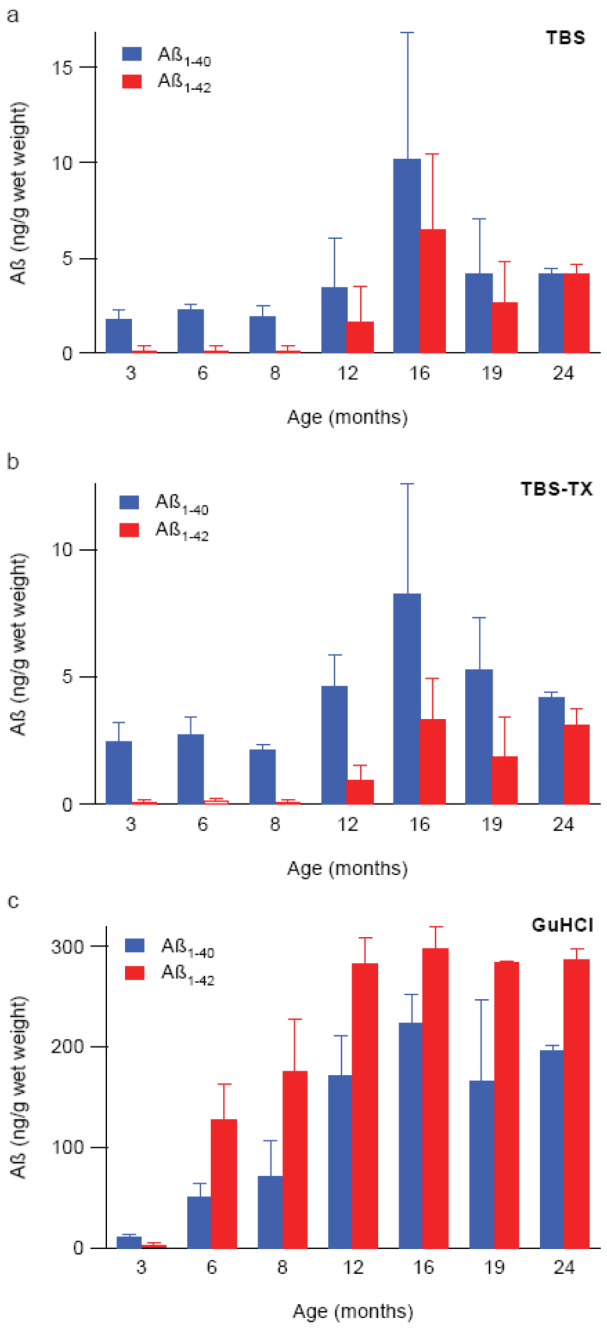

Figure 2. $A\beta_{1–40}$ is the predominant Aβ isoform present in aqeous extracts of J20 brain

Mouse brains were sequentially homogenized in (a) TBS, (b) TBS + 1% TX-100, and (c) GuHCl (see Methods). $A\beta_{1–40}$ (blue) and $A\beta_{1–42}$ (red) in these extracts were quantified by ELISA. In TBS and TBS-TX extracts $A\beta_{1–40}$ was the major species whereas $A\beta_{1–42}$ was the dominant species detected in the GuHCl extracts. Values shown are the mean of averaged individual animal values +/− standard deviation of the group mean. The number of animals analyzed in each age group varied between 2 and 6, with n=6 for 3, 6, 8 and 16 months; n=5 for 12 months and n=2 for both 19 and 24 months.

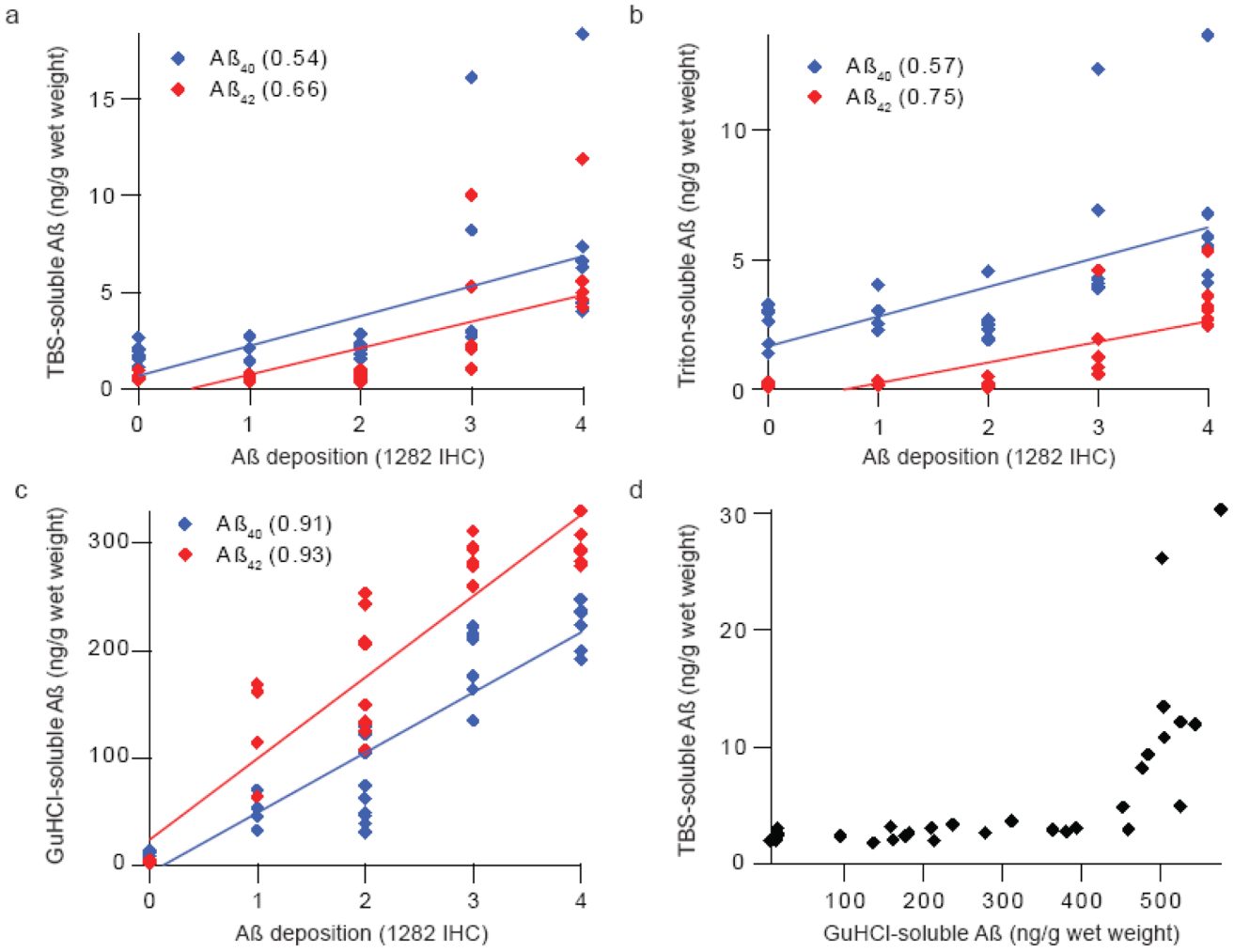

Figure 3. The concentration of Aβ in GuHCl extracts strongly correlates with amyloid burden detected by immunohistochemistry

Semi-quantitative estimates of amyloid burden (Table 1) were plotted against ELISA-determined concentrations of $A\beta_{40}$ (blue) and $A\beta_{42}$ (red) from (a) TBS or (b) TBS-TX and (c) GuHCl extracts. While GuHCl-soluble Aβ displays a strong linear correlation with amyloid burden (c), (d) TBS-soluble Aβ displays supralinear increases after GuHCl-extracted Aβ concentration surpasses 450 ng/g wet brain weight. Best fit lines were generated using Igor Pro (WaveMetrics, Lake Oswego, OR) and r^2 values are provided. A total of 31 mice were used in this analysis. The number of animals with IHC scores = 0, +1, +2, +3 and +4 were 6, 4, 9, 6 and 6, respectively.

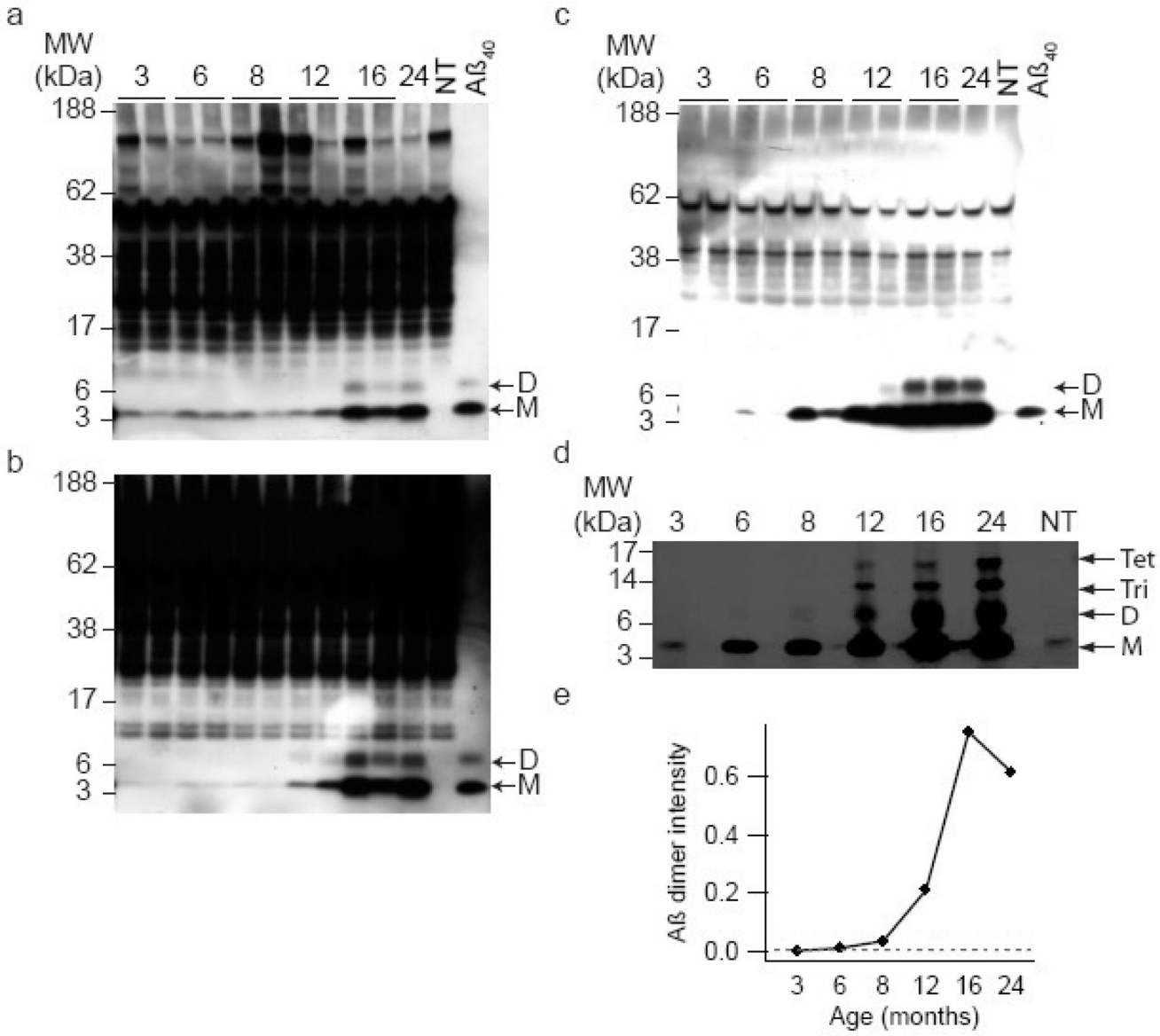

Figure 4. SDS-stable low-n oligomers of Aβ are detected in J20 brain

Representative Western blots of IPs from a total of 11 mouse brain homogenates are shown. (a) TBS, (b) TBS-TX, and (c) GuHCl extracts were IP'ed with the polyclonal anti-Aβ antibody, R1282, subjected to SDS-PAGE and detected with a combination of the anti-Aβ40 and Aβ42 monoclonal antibodies 2G3 and 21F12. An age-dependent increase in the concentration of Aβ monomers (M) and dimers (D) is observed in all three extracts. (d) When four times the volume of GuHCl material used in (c) was analyzed, Aβ dimmers could be faintly detected as early as ~8 months. Use of larger volumes of GuHCl extract for IP also revealed Aβ trimers (Tri) and tetramers (Tet) beginning at ~12 months. (e) Densitometric analysis of the ~8 kDa dimer band detected in (d) suggests that Aβ dimmer first appears between ~6–8 months. NT indicates samples from non-transgenic mice and Aβ40 indicates synthetic human Aβ1–40.

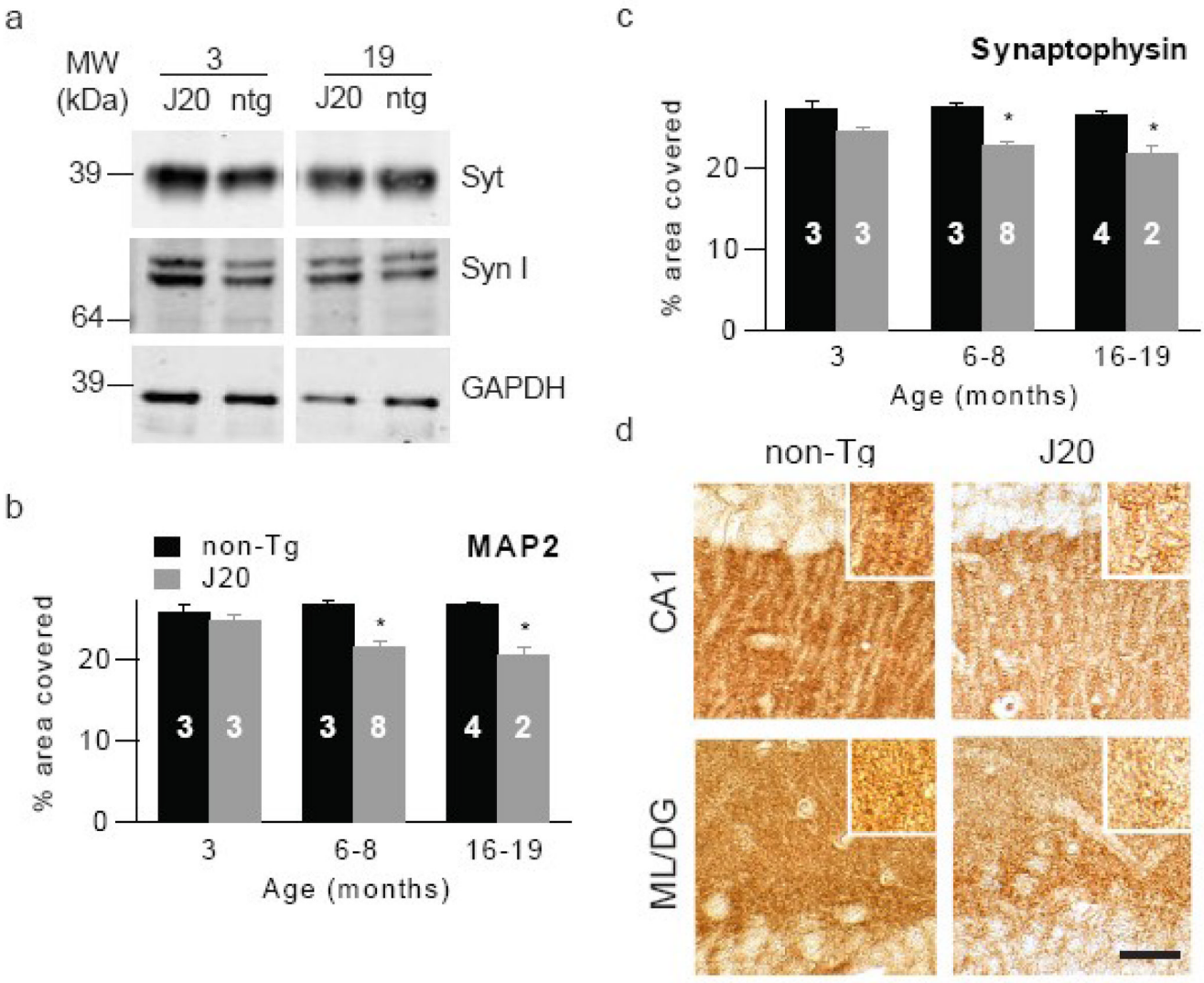

Figure 5. Immunohistochemical analysis of the hippocampus reveals an early and age-dependent increase in neuritic dystrophy in the absence of detectable changes in whole brain homogenates

(a) Representative W/blots of TBS-TX extracts probed with antibodies for synaptophysin (Syt) or synapsin I (Syn I). reveal no significant differences between similarly aged J20 and non-transgenic mice. Sagittal sections of hippocampus were stained with antibodies against (b) MAP2 or (c) synaptophysin and staining quantified as percent area covered. Both MAP2 and synaptophysin density decreased with age in J20 mice. The number of animals in each group are indicated on the histograms in white text. Representative images depicting synaptophysin immunostaining in the CA1 of the hippocampus and mid-molecular layer of the dentate gyrus of 6–8 month old non-transgenic and J20 mice are shown. Scale bar =20 μM.

Neurobiol Dis. Author manuscript; available in PMC 2010 November 1.

Table 1

Age-dependent increases in amyloid deposition and markers of neuritic dystrophy.

Genotype	Age (mo)	R1282 (Aβ)	BS42 (Aβ42)	A11 (oligomer)	8E5* (APP)	AT8 (p-Tau)	CD45 (microglia)
J20	3	–	–	–	–	–	–
J20	3	–	–	–	–	–	–
J20	3	–	–	–	–	–	–
J20	3	–	–	–	–	–	–
J20	3	–	–	–	–	–	–
J20	3	–	–	–	NA	–	–
J20	3	–	–	–	–	–	–
wt	3						
wt	3	–	–	–	–	–	–
wt	3	–	–	–	–	–	–
wt	3	–	–	–	–	–	–
wt	3	–	NA	–	–	–	–
wt	3	NA	–	–	–	–	–
J20	6	2+	1+	1+	1+	–	1+
J20	6	1+	1+	1+	–	–	1+
J20	6	1+	–	1+	–	–	–
J20	6	1+	1+/–	1+	1+	–	1+
J20	6	2+	1+	2+	1+	1+	2+
J20	6	2+	1+	1+	1+	–	1+
J20	8	2+	1+	1+	1+	–	1+
J20	8	2+	1+	1+	1+	–	2+
J20	8	1+	1+	1+	–	–	1+
J20	8	2+	1+	1+	1+	1+	1+
J20	8	2+	1+	1+	1+	–	2+
J20	8	2+	NA	2+	1+	NA	1+
J20	12	3+	2+	2+	2+	–	2+
J20	12	3+	2+	1+	2+	NA	1+
J20	12	3+	3+	2+	2+	1+	3+
J20	12	2+	2+	2+	1+	1+	1+
J20	12	3+	2+	2+	2+	–	2+
wt	16	–	–	2+	–	–	–
J20	15	3+	2+	2+	2+	1+	3+
J20	17	3+	3+	1+	1+	NA	2+
J20	17	4+	4+	3+	2+	1+	3+
J20	18	4+	1+	2+	2+	–	2+
J20	18	4+	2+	2+	2+	–	1+
J20	20	4+	3+	2+	2+	1+	2+
J20	20	NA	NA	NA	NA	NA	NA
J20	20	NA	NA	NA	NA	NA	NA
wt	18	NA	–	1+	–	–	–
wt	18	–	–	1+	–	–	–
wt	20	–	–	–	–	–	–
J20	24	4+	3+	2+	1+	1+	1+
J20	24	4+	3+	2+	2+	1+	3+

NA = not analyzed, – = no staining, + = detectable staining, increasing in intensity proportional to the numeric value.

*8E5 immunoreactivity refers to dystrophic neuritis only.